Organic & Biomolecular Chemistry

ROYAL SOCIETY OF CHEMISTRY

PAPER

View Article Online
View Journal | View Issue

Cite this: *Org. Biomol. Chem.*, 2025, **23**, 5380

Viscosity effects on the chemiluminescence emission of 1,2-dioxetanes in water†

Maidileyvis Castro Cabello, Palanisamy Kandhan, Peng Tao and Alexander R. Lippert *

Received 12th February 2025,
Accepted 1st May 2025

DOI: 10.1039/d5ob00254k

rsc.li/obc

Chemiluminescence emission from 1,2-dioxetanes offers a versatile framework for molecular imaging in cells and animals. Here, we observe an increase in chemiluminescence emission intensity with increasing solvent viscosity in aqueous systems, and interpret these observations within the context of chemically initiated electron exchange luminescence (CIEEL), concerted charge transfer induced luminescence (CTIL), and gradually reversible charge transfer induced luminescence (GR-CTIL) mechanisms.

Introduction

Chemiluminescence is the emission of light from an electronic excited state accessed in the course of a chemical reaction without photon absorption.[1] The triggered decomposition of sterically stabilized 1,2-dioxetanes is a chemiluminescence reaction that has been particularly useful for bioimaging[2,3] and other applications.[4–6] Early demonstrations that 1,2-dioxetanes are biocompatible with emissions bright enough to observe through living tissue[7–9] have sparked world-wide research activity in this area.[2,3,10,11,12–15] Steric stabilization of 1,2-dioxetanes prevents rapid thermal chemiluminescence decomposition.[1] However, installation of a phenolate *meta* to the 1,2-dioxetane can trigger chemiluminescence.[16–18] Several mechanisms have been proposed including chemically initiated electron exchange luminescence mechanism (CIEEL),[19] charge transfer induced luminescence (CTIL),[20] and gradually reversible charge transfer induced luminescence (GR-CTIL).[21] Mechanistic studies on the chemiluminescence decomposition of 1,2-dioxetanes have been performed in organic media and a likely pathway involves rate-limiting electron or charge transfer from the phenolate to the dioxetane as supported by empirical Hammett analyses[22] and multiconfigurational computational methods.[21]

The CIEEL mechanism proceeds *via* further cleavage of the carbon–carbon bond to form a radical pair in a solvent cage, and then electron back transfer to generate the phenolate in the excited state (Scheme 1). Empirical evidence for the electron back transfer chemiexcitation step was initially gathered in organic media by measuring chemiluminescent quantum yields in response to varying the viscosity of the solvent medium.[23,24–26] This data has been analysed in terms of a collisional model, where the increase in quantum yield with increasing viscosity is interpreted as evidence for a solvent cage because increasing viscosity will reduce the rate of cage escape and increase the yield of electron back transfer products.[23,26] A similar free-volume model interprets the electron back transfer steps in terms of molecular reorganization.[25,26] These types of viscosity studies in organic media have been executed on spiroadamantane 1,2-dioxetanes,[23,24,26] bicyclic dioxetanes,[25,26] diphenoyl peroxide,[27,28] 1,2-dioxetanones,[27,28] and the peroxyoxalate chemiluminescent reaction.[26]

A related mechanism with concerted intramolecular electron back transfer and C–C bond cleavage has been invoked to explain high singlet quantum yields and observed viscosity effects.[26] The charge-transfer induced luminescence (CTIL) mechanism was proposed as a concerted path for dioxetane luminescence,[20] as well as a more recent stepwise gradually reversible charge transfer induced luminescence mechanism (GR-CTIL),[21] which posits that partial charge transfer occurs instead of full charge transfer.

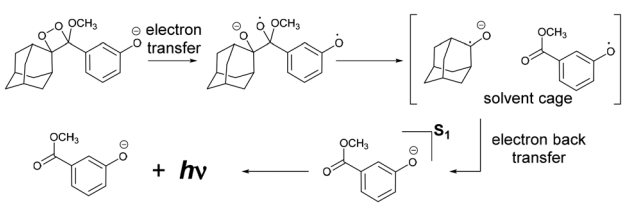

Scheme 1 Chemically initiated electron exchange luminescence (CIEEL) mechanism with chemiexcitation occurring with electron back transfer of a solvent-caged radical pair.

Department of Chemistry, Southern Methodist University, Dallas, TX 75275-0314, USA. E-mail: alippert@smu.edu

† Electronic supplementary information (ESI) available: Experimental procedures and supplementary figures. See DOI: https://doi.org/10.1039/d5ob00254k

Despite this body of mechanistic work in organic media, most imaging applications using modern 1,2-dioxetanes are performed in aqueous systems, especially since the disclosure of elegant synthetic modifications reported by Shabat and co-workers that drastically increase fluorescence and chemiluminescence quantum yields in water.[29,30] Strikingly, the mechanistic roles of electron back transfer and/or charge transfer have never been systematically investigated for these high quantum yield dioxetanes in aqueous systems.

This study serves to bridge this critical knowledge gap by investigating the mechanism of chemiluminescence decomposition of 1,2-dioxetanes in aqueous conditions. Herein, we studied the decomposition of mono- and bicyclic 1,2-dioxetanes **1** and **2** (Scheme 2) in PBS (pH = 7.4) at different viscosities using polyethylene glycol (PEG-3350) and ethylene glycol (EG). The rationale for using two different solvents to modulate viscosity is to have two independent experimental systems that can increase confidence if the two systems show similar correlations with viscosity. For both systems, the singlet quantum yield increases with solvent viscosity, providing empirical mechanistic evidence in aqueous systems that we have interpreted using several mechanistic models.

Results

A monocyclic dioxetane **1**, consisting of a spiroadamantane stabilized 1,2-dioxetane, and a bicyclic dioxetane **2**, were synthesized using adaptations of previous procedures (Schemes 2, S1 and S2†).[31,32] Both of these dioxetanes have excellent thermal stability (>1 year),[33] enabling distinction between thermal mechanisms and electron transfer or charge transfer mechanisms. The isopropyl group on **2** was chosen *versus* a *tert*-butyl group due to the commercial availability of the diol precursor 2,2,4-trimethyl-1,3-pentanediol (Scheme S1†). Viscosity effects on the chemiluminescence decomposition of both dioxetanes were studied using 100 mM phosphate buffered saline (PBS) at pH 7.4 and using mixtures of PBS with polyethylene glycol (PEG-3350) or ethylene glycol (EG) to increase solvent viscosity. Similar aqueous mixtures have previously been used to investigate the role of a solvent caged radical pair in reactions of peroxynitrite.[34,35] Experiments were carried out using 1.33% of DMSO as a practical matter for preparing solutions from a standard stock solution of the dioxetanes in DMSO. The viscosities for each of these solvent mixtures was measured using an Ostwald capillary viscometer, and these values are tabulated in Table S1.† The average kinetic traces of the chemiluminescence emission resulting from the decomposition of **1** and **2** are shown in Fig. 1. Increasing from 0% to 30% PEG-3350 results in a slower rate of chemiluminescence decomposition and an increase in total light emission for both dioxetanes **1** (Fig. 1A) and **2** (Fig. 1C), showing that viscosity influences both the emission intensity and emission kinetics. A similar trend is seen for increasing the amount of ethylene glycol (Fig. 1B and D). The observed rate constants were obtained by fitting these intensity *versus* time curves using mono exponential decay functions for dioxetanes **1** (Fig. S2,† and Table 1) and **2** (Fig. S3,† and Table 2).

The singlet chemiexcitation quantum yields (Φ_s) can be determined from the observed chemiluminescence quantum yield (Φ_{CL}) divided by the fluorescence quantum yield (Φ_{fl}) according to eqn (1).

$$\Phi_s = \Phi_{CL}/\Phi_{fl} \quad (1)$$

Authentic emitters **3** and **4** were independently synthesized and isolated and the fluorescence quantum yields (Φ_{fl}) in the different solvent mixtures were determined using an integrating sphere (Fig. 2). The fluorescence quantum yield of **3** (the authentic emitter for **1**) shows an increase as the viscosity increases (Fig. 2A), while **4** (the authentic emitter of **2**) does not depend on viscosity, and displays a constant average value of 0.515 over the entire range (Fig. 2B).

These fluorescence quantum yields are tabulated in Table S2.† The chemiluminescence quantum yields (Φ_{CL}) were determined from the integration of the curves using luminol as a standard (Fig. 3A, B and Tables 3, 4),[36] and the singlet quantum yields (Φ_s) are calculated according to eqn (1) (Fig. 3C, D, and Tables 5, 6). For both dioxetanes **1** and **2**, increases in

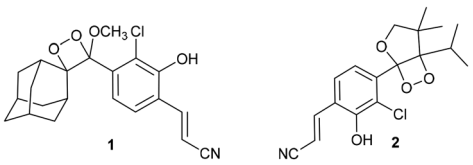

Scheme 2 Structure of the monocyclic dioxetane **1** and bicyclic dioxetane **2**.

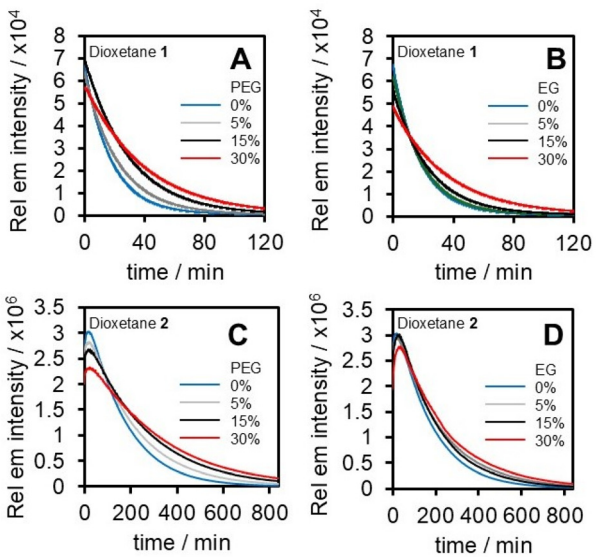

Fig. 1 Average kinetic emission intensity profiles for the decomposition of (A) 0.66 μM **1** and (C) 10 μM **2** in different mixtures of PBS/PEG-3350, and (B) 0.66 μM **1** and (D) 10 μM **2** in different mixtures of PBS/EG (ethylene glycol). Error bars (S.D. of n = 3 technical replicates) are removed for clarity but can be found in Fig. S1.†

Table 1 Effect of viscosity on the emission decay rate constant (k_{obs}) in the decomposition of 0.66 μM monocyclic 1,2-dioxetane **1** at 25 °C in 100 mM PBS (pH 7.4) with 1.3% DMSO

	PEG-3350		EG	
wt%	cP	k_{obs} (s^{-1})	cP	k_{obs} (s^{-1})
0	0.89	$0.937 \pm 0.003 \times 10^{-3}$	0.89	$0.937 \pm 0.005 \times 10^{-3}$
5	1.58	$0.729 \pm 0.007 \times 10^{-3}$	1.11	$0.862 \pm 0.004 \times 10^{-3}$
15	4.32	$0.559 \pm 0.007 \times 10^{-3}$	1.47	$0.700 \pm 0.005 \times 10^{-3}$
30	10.16	$0.419 \pm 0.002 \times 10^{-3}$	2.15	$0.458 \pm 0.007 \times 10^{-3}$

Table 2 Effect of viscosity on the emission decay rate constant (k_{obs}) in the decomposition of 10 μM bicyclic 1,2-dioxetane **2** at 25 °C in 100 mM (pH = 7.4) with 1.3% DMSO

	PEG-3350		EG	
wt%	cP	k_{obs} (s^{-1})	cP	k_{obs} (s^{-1})
0	0.89	$0.922 \pm 0.008 \times 10^{-4}$	0.89	$1.04 \pm 0.02 \times 10^{-4}$
5	1.58	$0.781 \pm 0.009 \times 10^{-4}$	1.11	$0.99 \pm 0.01 \times 10^{-4}$
15	4.32	$0.611 \pm 0.006 \times 10^{-4}$	1.47	$0.879 \pm 0.004 \times 10^{-4}$
30	10.16	$0.472 \pm 0.004 \times 10^{-4}$	2.15	$0.725 \pm 0.004 \times 10^{-4}$

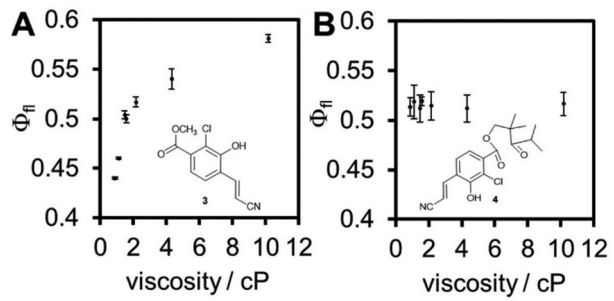

Fig. 2 Viscosity dependence of the fluorescence quantum yield of the authentic emitters (A) **3** and (B) **4** from the decomposition of **1** and **2** in different mixtures of PBS/EG and PBS/PEG-3350, at 25 °C.

the chemiluminescence quantum yield (Φ_{CL}) and singlet quantum yield (Φ_s) are observed as the viscosity of the medium is increased. The total Φ_s values increase by a factor of 1.34 and 1.30 in response to a 11.4-fold viscosity increase for the decomposition of **1** and **2** respectively. Importantly, the data for PEG-3350 (PEG, Fig. 3 blue data points) and ethylene glycol (EG, Fig. 3 red data points) fall along the same curve, providing confidence that the effects are indeed due to changes in solvent viscosity. Additionally, the polarity of the solvent mixtures was measured using Reichardt's dye and was found to be relatively constant, providing further support to conclude that the observed differences are due to viscosity (Fig. S3†). It is noteworthy that dioxetane **1** reaches a singlet quantum yield (Φ_s) near unity in highly viscous medium, highlighting the excellent performance of this dioxetane. Tables 3–6 summarize the measured chemiluminescence and singlet quantum yields for dioxetanes **1** and **2** in these solvent systems.

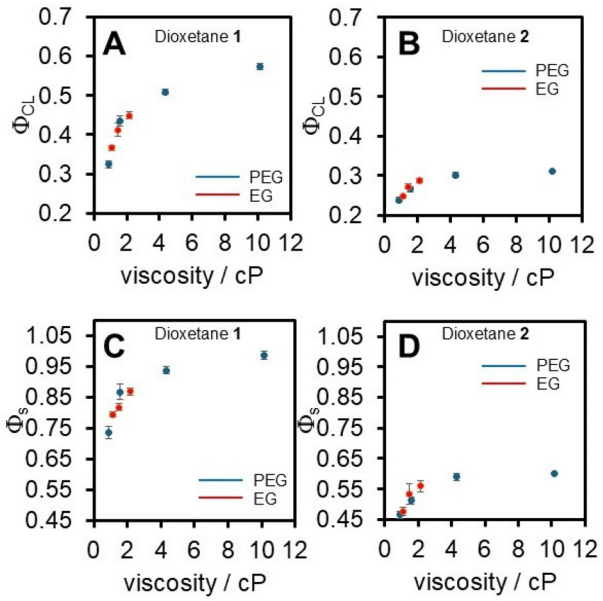

Fig. 3 Viscosity dependence of the (A) and (B) chemiluminescence quantum yield of the decomposition of (A) dioxetane **1** and (B) dioxetane **2**, and (C) and (D) the singlet quantum yield (Φ_s) of the decomposition of (C) dioxetane **1** and (D) dioxetane **2** in different mixtures of PBS/EG (red data points) and PBS/PEG-3350 (blue data points), at 25 °C.

Table 3 Effect of viscosity on the chemiluminescence quantum yield (Φ_{CL}) in the decomposition the decomposition of 0.66 μM monocyclic 1,2-dioxetane **1** at 25 °C in 100 mM PBS (pH 7.4) with 1.3% DMSO

	PEG-3350		EG	
wt%	cP	Φ_{CL}	cP	Φ_{CL}
0	0.89	0.32 ± 0.01 E mol^{-1}	0.89	0.32 ± 0.01 E mol^{-1}
5	1.58	0.43 ± 0.01 E mol^{-1}	1.11	0.37 ± 0.01 E mol^{-1}
15	4.32	0.51 ± 0.01 E mol^{-1}	1.47	0.41 ± 0.02 E mol^{-1}
30	10.16	0.57 ± 0.01 E mol^{-1}	2.15	0.44 ± 0.01 E mol^{-1}

Table 4 Effect of viscosity on the chemiluminescence quantum yield (Φ_{CL}) in the decomposition the decomposition of 10 μM bicyclic 1,2-dioxetane **2** at 25 °C in 100 mM (pH = 7.4) with 1.3% DMSO

	PEG-3350		EG	
wt%	cP	Φ_{CL}	cP	Φ_{CL}
0	0.89	0.24 ± 0.01 E mol^{-1}	0.89	0.24 ± 0.01 E mol^{-1}
5	1.58	0.27 ± 0.01 E mol^{-1}	1.11	0.25 ± 0.004 E mol^{-1}
15	4.32	0.30 ± 0.01 E mol^{-1}	1.47	0.27 ± 0.01 E mol^{-1}
30	10.16	0.31 ± 0.001 E mol^{-1}	2.15	0.29 ± 0.006 E mol^{-1}

Discussion

Collisional and free-volume models

The behaviour of the chemiexcitation quantum yields with medium viscosity has been previously interpreted using collisional[23,24] and free-volume models,[25,26,37] which we have

Table 5 Effect of viscosity on the singlet quantum yield (Φ_s) in the decomposition the decomposition of 0.66 μM monocyclic 1,2-dioxetane **1** at 25 °C in 100 mM PBS (pH 7.4) with 1.3% DMSO

	PEG-3350		EG	
wt%	cP	Φ_s	cP	Φ_s
0	0.89	0.74 ± 0.02 E mol^{-1}	0.89	0.73 ± 0.03 E mol^{-1}
5	1.58	0.87 ± 0.03 E mol^{-1}	1.11	0.79 ± 0.01 E mol^{-1}
15	4.32	0.94 ± 0.01 E mol^{-1}	1.47	0.82 ± 0.03 E mol^{-1}
30	10.16	0.99 ± 0.01 E mol^{-1}	2.15	0.87 ± 0.02 E mol^{-1}

Table 6 Effect of viscosity on the singlet quantum yield (Φ_s) in the decomposition the decomposition of 10 μM bicyclic 1,2-dioxetane **2** at 25 °C in 100 mM (pH = 7.4) with 1.3% DMSO

	PEG-3350		EG	
wt%	cP	Φ_s	cP	Φ_s
0	0.89	0.46 ± 0.01 E mol^{-1}	0.89	0.46 ± 0.01 E mol^{-1}
5	1.58	0.51 ± 0.01 E mol^{-1}	1.11	0.48 ± 0.007 E mol^{-1}
15	4.32	0.58 ± 0.01 E mol^{-1}	1.47	0.53 ± 0.01 E mol^{-1}
30	10.16	0.60 ± 0.003 E mol^{-1}	2.15	0.56 ± 0.01 E mol^{-1}

used to analyse the data acquired in this study (Fig. 4). The collisional model is framed in terms of the probability of electron back transfer each time the molecular fragments collide within a solvent cage. A double reciprocal plot of singlet quantum yield and viscosity gives eqn (2),[23,26] with the parameters $B = p_{ebt}/p_{s1}$ and $A = A_n/p_{s1}$, enabling estimates of p_{s1}, the probability of obtaining the S_1 product per collision and p_{ebt} the probability of electron back transfer per collision, given knowledge of A_n, the Arrhenius preexponential factor for viscosity.[23] The values determined for these parameters are given in Table 7.

$$1/\Phi_s = B + A/\eta \quad (2)$$

A plot of $\ln \eta$ *versus* $1/T$ for PBS buffers containing increasing amounts of PEG-3350 gives Arrhenius plots for these solvent mixtures (Table S4, and Fig. S4†).[38] From these plots shown in Fig. S4,† the *y*-intercept is equal to $\ln A_n$, which is the Arrhenius preexponential factor for the viscosity, and we determined an average $A_n = 1.46 \pm 1.10 \times 10^{-3}$ cP from temperature dependent plots of PBS/PEG-3350 solvent mixtures. Using this value, we can estimate a probability of obtaining the singlet excited state product per collision within the solvent cage (from the expression $A = A_n/p_{s1}$) for **1** and **2** to be $p_{s1} = 4.6 \pm 3.6 \times 10^{-3}$ and $p_{s1} = 2.8 \pm 2.2 \times 10^{-3}$, respectively. This, in turn, allows us to estimate the probability of electron back transfer (from the expression $B = p_{ebt}/p_{s1}$) for **1** and **2** to be $p_{ebt} = 4.47 \pm 3.40 \times 10^{-3}$ and $4.46 \pm 3.40 \times 10^{-3}$. This collisional model interestingly suggests that while the probability of electron back transfer is essentially the same for **1** and **2**, the probability of entering the singlet state is about 60% more likely for **1** than **2**. This is consistent with dioxetane **1** reaching a Φ_s near unity at high viscosity, while the dioxetane **2** reaches a $\Phi_s = 0.6$, even at the highest viscosity tested. This analysis assumes that the yield of the solvent-caged radical pair (which we denote ϕ_{rp}) in the first step of the mechanism is 100%. We will relax this assumption in the derivation of a revised "cage-escape" model below. Additionally, we note that dioxetane **2** cannot undergo cage escape in a strict sense, so this mechanistic model should be interpreted as a separation of the radical pair through molecular reorientation, which is better modelled through the free-volume model described below.

The free-volume model relates the viscosity of the medium to the fraction of free volume needed to account for molecular motions through the free volume. This model is described by a plot using eqn (3) (Fig. 6C and D).[25,26,37]

$$\ln((1 - \Phi_s)/\Phi_s) = C - \alpha \ln(\eta) \quad (3)$$

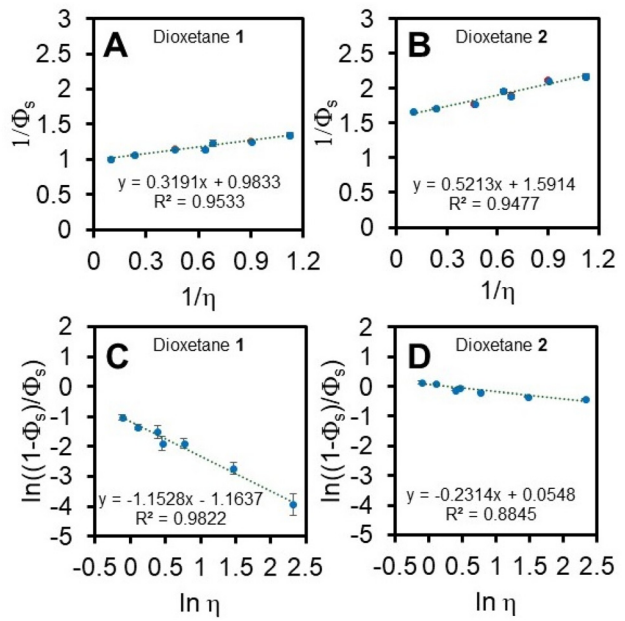

Fig. 4 Analysis of the singlet quantum yield of the decomposition of the 1,2-dioxetanes in different mixtures of PBS/EG and PBS/PEG-3350 using a collisional model for (A) dioxetane **1** and (B) dioxetane **2** or a free-volume model for (C) dioxetane **1** and (D) dioxetane **2**.

Table 7 Fitting parameters for the decomposition of 1,2-dioxetanes using two different models

	Collisional model: $1/\Phi_s = B + A/\eta$			Free-volume model: $\ln((1 - \Phi_s)/\Phi_s) = C - \alpha \ln \eta$		
	B	A	R^2	C	$-\alpha$	R^2
1	0.98	0.32	0.953	−1.16	1.15	0.982
2	1.59	0.52	0.948	0.05	0.23	0.885
3[26]	1.8	2.2	0.985	1.9	0.7	0.989
4[26]	7.8	4.1	0.93	2.4	0.3	0.98
5[26]	2.7	4.8	0.99	1.1	0.7	0.984
6[27]	10 000	14 000	0.89	10.11	0.5	0.96
7[27]	3200	1000	0.89	8.35	0.22	0.96
8[26]	−92	279	0.913	5.1	1.5	0.974

The parameter $-\alpha$ has been interpreted as the fraction of the free volume needed for a particular process, with $-\alpha < 1$ being indicative that molecular bond rotations are needed for the process to occur, and $-\alpha \sim 1$ has been interpreted as translational movement of the entire molecule in a bimolecular process.[25,26,37] We find that the monocyclic compound **1** has $-\alpha = 1.15$, a value that has been interpreted as a bimolecular process, while bicyclic compound **2** has $-\alpha = 0.23$, indicating that approximately a quarter of the free volume of the molecule is involved in viscosity-dependent processes, most likely bond rotations that change the molecular conformation. This result is consistent with $-\alpha$ values found for similar dioxetanes (mono and bicyclic) in organic solvents, albeit with a smaller $-\alpha$ of 0.7 found for the TBAF-initiated chemiluminescence for the monocyclic dioxetane **3**, and a comparable $-\alpha$ of 0.3 for the bicyclic dioxetane **4** in organic solvent (Table 7, and Fig. 5).[25,26] The dimethyl dioxetane **5** gave an $-\alpha$ of 0.7, similar to the spiroadamantane dioxetane **3**.[26] Bimolecular activated chemiluminescence systems have also been studied with regards to their viscosity dependence, including dioxetanone **6** and diphenoyl peroxide **7**,[27] which were activated by rubrene, and the peroxyoxalate chemiluminescent reaction using diphenyl anthracene as an activator. The dioxetanone and diphenyl peroxide systems gave smaller $-\alpha$ values of 0.5 and 0.22, respectively, while the peroxyoxalate system gives a $-\alpha$ of 1.5 (Table 7 and Fig. 5, **6–8**).[26]

Cage escape and molecular reorganization models

One drawback of these models is that they implicitly assume that the yield of radical pair formation (ϕ_{rp}) is 100%, and observed singlet quantum yields of less than 100% are due to either a "direct" concerted pathway of chemiluminescence (not accounted for in the above treatment) or due to formation of non-emissive singlet ground states or triplet excited states. We have thus reinterpreted the data for these compounds in terms of revised models where the yield of formation of a radical pair is taken into consideration (eqn (4)), where ϕ_{rp} is the yield of the radical pair and ϕ_{ebt} is the yield of electron back transfer to the singlet excited state (Scheme 3).

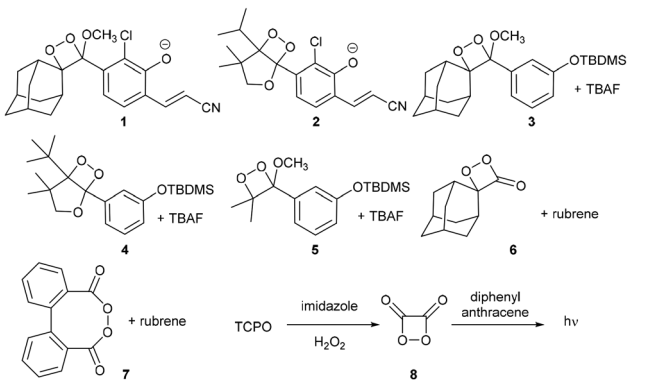

Fig. 5 Summary of chemiluminescence systems that have been studied using viscosity-dependence experiments.

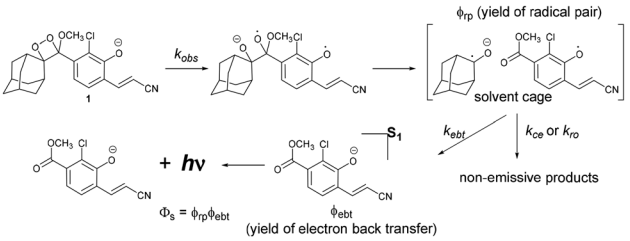

Scheme 3 Cage escape and molecular reorientation kinetic models.

$$\Phi_s = \phi_{rp}\phi_{ebt} \quad (4)$$

In a model that we describe as a "cage-escape" model, we assume that cage escape obeys the Eigen equation,[39] which states that rate of cage escape is proportional to η^{-1}. The yield of electron back transfer to the singlet excited state can be expressed in terms of the rate of electron back transfer (k_{ebt}) and the rate of cage escape (k_{ce}) (eqn (5)), with $k_{ce} = C_{ce}/\eta$ (eqn (5)), where C_{ce} comprises the constant terms of the Eigen equation (see ESI eqn (S9)–(S11)†). These equations can be combined and rearranged to give the double reciprocal eqn (7). Substituting eqn (4) into eqn (7) gives eqn (8) after simplification. A more detailed derivation can be found in the ESI.†

$$\phi_{ebt} = \frac{k_{ebt}}{k_{ebt} + k_{ce}} \quad (5)$$

$$k_{ce} = \frac{C_{ce}}{\eta} \quad (6)$$

$$\frac{1}{\phi_{ebt}} = 1 + \frac{C_{ce}}{k_{ebt}\eta} \quad (7)$$

$$\frac{1}{\Phi_s} = \frac{1}{\phi_{rp}} + \frac{C_{ce}}{\phi_{rp}k_{ebt}\eta} \quad (8)$$

This cage-escape model allows reinterpretation of the double reciprocal plots to give the yield of the radical pair formation ($\phi_{rp} = 1/B$) and relative rates of electron back transfer and cage escape ($k_{ebt}/k_{ce} = A \times \phi_{rp}/\eta$), the derivation of which is shown in ESI eqn (S20)–(S24)† by substituting $C_{ce} = \eta \times k_{ce}$ obtained from eqn (6) into the parameter $A = C_{ce}/\phi_{rp}k_{ebt}$. These values are summarized in Table 8. This model provides insight regarding the observed singlet quantum yields in various systems. For 1,2-dioxetanes, this model estimates high yields of radical pair formations as high as 100% and 63% for the case free phenolate dioxetanes **1** and **2**, and somewhat lower yields between 13–55% for the TBAF induced decomposition of **3–5**. This is in stark contrast with the intermolecular activation of dioxetanone **6** and diphenoyl peroxide **7** with rubrene, which the cage-escape model estimates for radical pair formation yields are 0.01% and 0.03%, respectively. This interpretation explains the differences in chemiluminescence emission between the intramolecular activation and intermolecular activation is largely due to differences in the yield of the radical pair formation, which is reasonable considering the intermolecular systems require the chemiluminescent compound

Table 8 Fitting parameters for the decomposition of 1,2-dioxetanes using reinterpreted cage escape and reorientation models

	Cage escape model: $\frac{1}{\Phi_s}=\frac{1}{\phi_{rp}}+\frac{C_{ce}}{\phi_{rp}k_{ebt}\eta}$			Reorientation model: $\frac{1}{\Phi_s}=\frac{1}{\phi_{rp}}+\frac{C_{or}}{\phi_{rp}k_{ebt}\eta^{\alpha}}$			
	ϕ_{rp}	$\frac{k_{ebt}}{k_{ce}}$ [a] (low η)	$\frac{k_{ebt}}{k_{ce}}$ [b] (high η)	ϕ_{rp} [c]	α	$\frac{k_{ebt}}{k_{or}}$ [a] (low η)	$\frac{k_{ebt}}{k_{or}}$ [b] (high η)
1	1.0	2.7	6.6	1.0	1.19	2.8	7.9
2	0.63	2.7	6.6	0.62	1.16	2.9	8.1
3[26]	0.55	0.43	2.2	—	—	—	—
4[26]	0.13	1.1	4.6	—	—	—	—
5[26]	0.37	0.30	1.5	—	—	—	—
6[27]	0.0001	0.40	1.8	0.0001	1.14	0.38	2.1
7[27]	0.0003	1.8	8.2	0.0003	0.94	1.9	8.0
8[26]	n.d.	n.d.	n.d.	0.022	2.47	0.11	4.9

[a] η = 0.54–0.89 cp. [b] η = 2.15–0.89 cp. [c] For entries **6** and **7**, ϕ_{rp} was constrained to the values determined in the cage-escape model.

and activator to collide and not every collision will have the appropriate trajectory to for productive radical pair formation.

We note that the data for the peroxyoxalate reaction does not provide meaningful information with this cage-escape model, given the negative value for the parameter *B*. However, we have also considered a "reorientation" model, which is similar to the free-volume model in that it models the viscosity effect as limiting the rate molecular reorientation (k_{or}) that leads to structures that do not undergo electron back transfer to the singlet excited state (eqn (9)). Generally, the dependency of the rate of molecular reorientation depends on $\eta^{-\alpha}$ (determined empirically and in independently derived models),[40] as described in eqn (10). Using a similar approach as taken above (and described in more detail in the ESI†), we arrive at eqn (11).

$$\phi_{ebt}=\frac{k_{ebt}}{k_{ebt}+k_{or}} \tag{9}$$

$$k_{or}=\frac{C_{or}}{\eta^{-\alpha}} \tag{10}$$

$$\frac{1}{\Phi_s}=\frac{1}{\phi_{rp}}+\frac{C_{or}}{\phi_{rp}k_{ebt}\eta^{\alpha}} \tag{11}$$

We performed non-linear fits to this expression for dioxetanes **1** and **2**, and for **6**,[27] **7**,[27] and **8**[26] using raw data provided in the literature (ESI Fig. S5–S9†). This reorientation model provides similar estimates for ϕ_{rp} of **1** and **2** as does the cage escape model, but we also determine a ϕ_{rp} = 2.2% for the peroxyoxalate system reported by Bastos *et al.*[26] This model gives revised α values, which show less difference between monocyclic **1** and bicyclic **2** due to accounting for the differences in the overall high singlet quantum yield at high viscosity, reflective of different ϕ_{rp}. These revised models also provide estimates of the relative rates of electron back transfer *versus* cage escape (k_{ebt}/k_{ce} for the cage escape model) or *versus* molecular reorientation (k_{ebt}/k_{or}) for the molecular reorientation model. The dioxetanes **1** and **2** in this study show higher ϕ_{rp} as well as higher k_{ebt}/k_{ce} and k_{ebt}/k_{or} at low viscosity than other dioxetane systems studied. The differences between k_{ebt}/k_{ce} and k_{ebt}/k_{or} at low *versus* high viscosity, in combination with the α values, gives a quantitative description of the magnitude of the viscosity effect for each system. We note that these models do not consider electron back transfer pathways to form non-emissive ground state singlet and triplet products. Assuming that these processes are independent of viscosity, we can re-evaluate eqn (8) to give eqn (12) below, which accounts for loss of quantum yield from incomplete radical pair formation as well as loss due to viscosity-independent electron back transfer to non-emissive states. If we assume that ϕ_{rp} = 1 and all losses in singlet quantum yield are due to formation of non-emissive states, we get eqn (13), which can give estimates of the relative rates and yields of non-emissive electron back transfer processes. It is likely that both radical pair formation and electron back transfer to non-emissive states are processes that reduce chemiluminescence emission yields, although they cannot be readily differentiated using these models. However, when considering the intermolecular systems **6** and **7**, there is a clear argument for low yields of radical pair formation due to the likelihood of trajectory-dependent outcomes, specifically whether the collision brings the activator in contact with the O–O bond or not. In the cases of the intramolecular activation of 1,2-dioxetanes, the activator and dioxetane are pre-organized, and the 1,2-dioxetanedione high energy intermediate[41] of the peroxyoxalate system is symmetric and less sterically hindered. Therefore, it is reasonable to think that collisions in this system are more likely to result in radical pair formation, in line with previous arguments.[42,43]

$$\frac{1}{\Phi_s}=\frac{1+\frac{k_{ebt(S_0)}+k_{ebt(T_1)}}{k_{ebt(S_1)}}}{\phi_{rp}}+\frac{C_{ce}}{\phi_{rp}k_{ebt(S_1)}\eta} \tag{12}$$

$$\frac{1}{\Phi_s}=1+\frac{k_{ebt(S_0)}+k_{ebt(T_1)}}{k_{ebt(S_1)}}+\frac{C_{ce}}{k_{ebt(S_1)}\eta} \tag{13}$$

Concerted charge transfer induced luminescence (CTIL)

These revised models assume the formation of a solvent-caged radical pair, that can either undergo electron back transfer to the singlet excited state or a viscosity-dependent process (cage escape or molecular reorientation) that leads to a non-emissive product. However, other mechanistic pathways have been proposed based on empirical and theoretical studies.[20,21,26] A direct, concerted pathway from the dioxetane to the singlet excited state *via* a charge transfer intermediate is described as a charge transfer induced luminescence (CTIL) mechanism.[20] It is, however, difficult to explain the observed and reproducible viscosity dependence of the concerted path. One could invoke the need for a specific conformation of the aryl ring rotation for optimal charge transfer to occur, which would be viscosity dependent. A reduction in the rate is indeed observed with increasing viscosity, which could in principle be explained by viscosity hindering achieving an appropriate conformation for efficient charge transfer as supported by a com-

putational analysis below. However, while the kinetics of emission, which in a concerted CTIL mechanism would be in the same step as chemiexcitation, is decreased with increasing viscosity, the chemiluminescence quantum yield increases with increasing viscosity. If this were a concerted reaction, one would expect similar trends for the rate-limiting step and chemiluminescence emission. By contrast, a stepwise mechanism with distinct intermediates and kinetics could explain these differences.

Concerted electron back transfer and gradually reversible charge transfer induced luminescence (GR-CTIL)

Two stepwise mechanisms have been proposed that do not rely on intermolecular electron back transfer from a solvent-caged radical pair. A concerted electron back transfer and C–C bond cleavage after the formation of an initial full electron transfer biradical intermediate has been proposed,[26] with the viscosity effect interpreted as bond rotation of the initial radical pair to a conformation that does not undergo concerted formation of the singlet excited state (Fig. 6A). Our data can provide insight to this model for intramolecular electron back transfer. Dioxetanes **1** and **2** show similar k_{ebt}/k_{ce} and k_{ebt}/k_{or}, which could be expected if the intermediates after the initial electron transfer are similar as described in the CIEEL mechanism Scheme 3, which could be reasonably expected to have similar rates of electron back transfer *versus* molecular reorganization. On the other hand, the viscosity dependence (k_{or} and α values) is not as consistent with bond rotation around the C–C bond because dioxetane **2** is significantly more restricted due to the five-membered ring still being intact (Fig. 6B). An alternate bond rotation could be invoked by considering rotation around the C–C bond connecting the aryl ring and the dioxetane, which would indeed be similar for the two structures and could conceivably result in a similar viscosity effect on k_{or} and α values.

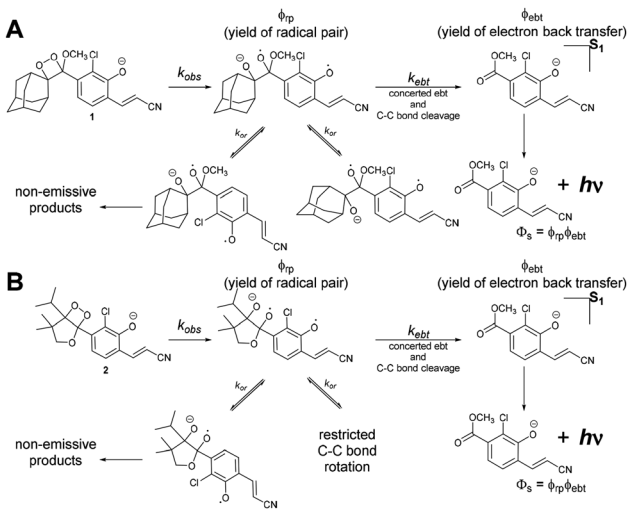

Fig. 6 Intramolecular concerted electron back transfer model.

In these models, the differences in singlet quantum yield between **1** and **2** would be explained either by differences in the yield of radical pair formation or differences in the ratio of electron back transfer to an emissive excited singlet state or a non-emissive ground singlet or triplet state. Differences in dioxetane ring strain could lead to differences in efficiency of the initial radical pair formation, ϕ_{rp}. This is consonant with an approximately 10-fold lower k_{obs} for **2** *versus* **1**, an indication that this first step may not be as efficient with other competitive processes.

A stepwise mechanism is also consonant with the gradually reversible charge transfer induced chemiluminescence (GR-CTIL).[21] Using multiconfigurational computational methods, a reaction pathway for the decomposition of 1,2-dioxetanes similar to **1** and **3** was computed that showed an initial charge transfer step to form a biradicaloid intermediate, followed by C–C bond cleavage, with a charge back transfer occurring after $S_0 \rightarrow S_1$ transition. Similarly to the concerted electron back transfer mechanism discussed above,[26] the viscosity-dependence of the chemiluminescence emission can be reasoned by a viscosity dependence of the bond rotation away from conformations that are optimal for $S_0 \rightarrow S_1$ cross-over. This is supported by the computed potential energy curves that indicate the bond rotation around the C–C bond is an important part of the reaction pathway.[21] The reorientation model can be used in this case, where k_{ebt} would be substituted with k_{C-C}, the rate of dioxetane C–C bond cleavage/chemiexcitation in the second step of the GR-CTIL mechanism. Thus, the derived molecular reorientation model could be applied in the context of a GR-CTIL mechanism to give useful estimates of ϕ_{rp} and relative rates of the $S_0 \rightarrow S_1$ chemiexcitation *versus* viscosity dependent molecular reorientation.

Viscosity effects on the rates of chemiluminescence emission

Viscosity effects are observed for both the kinetics of the chemiluminescence emission (which decrease with increasing viscosity), and the intensity of the chemiluminescence emission (which increases with increasing viscosity). In order to understand the decrease in the rate of the reaction with increasing viscosity, it is possible that a specific conformation with regards to the rotation around the aryl–dioxetane bond may be optimal for the initial electron transfer step. We computationally investigated how rotation around the aryl–dioxetane bond affected the global energy (to find the minimum energy conformation) and the HOMO–LUMO gap (to gain insight into the energy barrier for electron transfer).

The potential energy surface (PES) along the dihedral angles between the 1,2-dioxetane and aryl ring was constructed based on relaxed scan calculations for the ionized forms of both compounds **1** and **2** (Fig. 7A and B). Both compounds have two barriers associated with the rotation of the target dihedral angles. For compound **1**, these two barriers are 28 kcal mol^{-1} (with the dihedral angle at 74 degrees) and 20 kcal mol^{-1} at 274 degrees. For compound **2**, these two barriers are 14 kcal mol^{-1} at 145 degrees and 20 kcal mol^{-1} at 325 degrees. The structures with the lowest potential energy of both com-

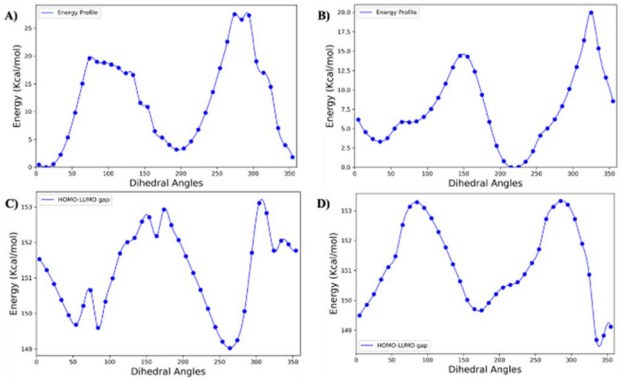

Fig. 7 (A) and (C) show the total energy and HOMO–LUMO energy gap as a function of dihedral angles for compound **1**. (B) and (D) show the total energy and HOMO–LUMO energy gap as a function of dihedral angles for compound **2**.

pounds **1** and **2** exhibit similar conformations in terms of the relative orientation between chlorine and 1,2-dioxetane groups (Fig. 8A and B). The dihedral angles for geometries with the lowest potential energy are 14 degrees and 215 degrees for compounds **1** and **2**, respectively.

For comparison, the HOMO–LUMO energy gap was analysed across all conformations to gain insight and compare dihedral angles of the minimum energy conformations to the conformations with the lowest HOMO–LUMO gap. The rotation between the 1,2-dioxetane and aryl rings significantly influenced the HOMO–LUMO energy gap for both compounds (Fig. 7C and D). The ranges of HOMO–LUMO energy gap for compounds **1** and **2** are roughly between 149 kcal mol^{-1} and 153 kcal mol^{-1} with compound **2** displaying slightly wider range. Interestingly, the geometries with the lowest HOMO–LUMO energy gap are different from the geometries with the lowest potential energy for both compounds (Fig. 8C and D). The dihedral angles for geometries with the lowest HOMO–LUMO energy gap are 264 degrees and 335 degrees for compounds **1** and **2**, respectively. Interestingly, the orientation of the chlorine in the structure with the lowest HOMO–LUMO energy gap is opposite from the structure with the lowest potential energy for both compounds.

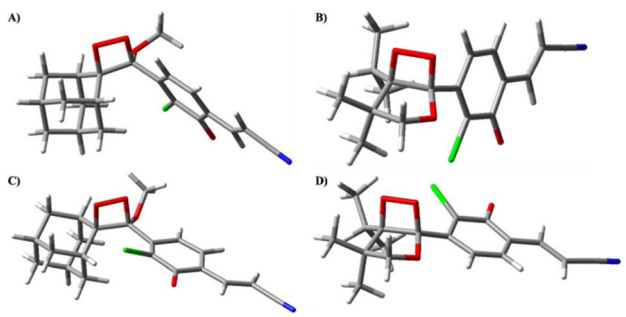

Fig. 8 Key geometries from relaxed scan calculations of compounds **1** and **2**. (A) The geometry of compound **1** with the lowest potential energy. (B) The geometry of compound **2** with the lowest potential energy. (C) The geometry of compound **1** with the lowest HOMO–LUMO energy gap. (D) The geometry of compound **2** with the lowest HOMO–LUMO energy gap.

These computations show the possibility that conversion from the lowest energy ground state conformation to the conformation with the lowest HOMO–LUMO gap requires a bond rotation, which would be expected to be viscosity dependent. While a full treatment of the reaction pathway using this relaxed scan approach is outside the scope of the current work, it provides a reasonable explanation of the viscosity dependence of the kinetics. We do note that the trends of these viscosity effects of k_{obs} differ between ethylene glycol and PEG-3350, in contradistinction to Φ_s, which shows similar viscosity dependence for ethylene glycol and PEG-3350. Therefore, caution should be exercised when interpreting the viscosity effects on k_{obs}.

Conclusions

This study demonstrates that dioxetanes **1** and **2** display clearly observable viscosity-dependent increases in chemiluminescence and singlet quantum yields. Singlet quantum yields at high viscosity approaching 100% for dioxetane **1** and 60% for dioxetane **2** were observed. Two strengths of the experimental approach include studying the system across a wide range of viscosity (~10-fold increase in viscosity) and using two solvent systems, ethylene glycol and PEG-3350, that show similar effects on chemiluminescence emission intensity at similar viscosities, increasing confidence that the effects of increasing concentrations of PEG-3350 or ethylene glycol are due to increasing viscosity and not due to other factors like solvent reorganization energy or solvent polarity. A decrease in k_{obs} is measured with increasing concentrations of ethylene glycol and PEG-3350, although trends are slightly different for these two solvent systems. We note that viscosity dependence on chemiluminescence has been reproducibly observed in several different laboratories and several chemiluminescence systems, so any mechanistic proposal should be consistent with these empirical observations.

We have analysed the data in the context of classic collisional and free-volume intermolecular CIEEL models, newly derived "cage-escape" and "molecular reorientation" kinetic models that consider the yield of radical pair formation, an intramolecular CIEEL model with concerted electron back transfer and C–C bond cleavage, concerted CTIL, and the stepwise GR-CTIL model. Differential viscosity effects where k_{obs} is decreased while Φ_s is increased with increasing viscosity is more consistent with a stepwise mechanism with distinct rate-limiting and chemiexcitation steps. Accounting for the yield of radical pair formation provides useful insights, in particular providing a rationalization for the high singlet quantum yields of dioxetanes with intramolecular activators (**1–5** in Fig. 5) *versus* the lower singlet quantum yields for systems that require intermolecular activation (**6–8** in Fig. 5), although we

note that the estimates of radical pair yields are not completely disentangled from other viscosity-independent processes that reduce Φ_s. These models can also give estimates of relative rates of pathways after the rate-limiting step by virtue of measuring differences in the fast chemiexcitation step of the mechanism. In summary, this study provides the first aqueous data for how viscosity effects chemiluminescence emission and mechanistic insights that will serve to inform future molecular design.

Author contributions

Maidileyvis Castro Cabello: writing – review & editing, writing – original draft, methodology, investigation, formal analysis, conceptualization. Palanisamy Kandhan: writing – review & editing, methodology, investigation, formal analysis. Peng Tao: writing – review & editing, methodology, investigation, formal analysis, supervision. Alexander R. Lippert: writing – review & editing, writing – original draft, supervision, project administration, funding acquisition, formal analysis, conceptualization.

Data availability

The data supporting this article have been included as ESI.†

Conflicts of interest

A.R.L. declares a financial stake in Biolum Science, LLC. The other authors have no conflicts to declare.

References

1 M. Vacher, I. F. Galván, B.-W. Ding, S. Schramm, R. Berraud-Pache, P. Naumov, N. Ferré, Y.-J. Liu, I. Navizet, D. Roca-Sanjuán, W. J. Baader and R. Lindh, Chemi- and Bioluminescence of Cyclic Peroxides, *Chem. Rev.*, 2018, **118**, 6927–6974.
2 U. Haris, H. N. Kagalwala, Y. Lisa Kim and A. R. Lippert, Seeking Illumination: The Path to Chemiluminescent 1,2-Dioxetanes for Quantitative Measurements and In Vivo Imaging, *Acc. Chem. Res.*, 2021, **54**, 2844–2857.
3 U. Haris and A. R. Lippert, Exploring the Structural Space of Chemiluminescent 1,2-Dioxetanes, *ACS Sens.*, 2022, **8**, 3–11.
4 K. A. Jones, K. Kentala, M. W. Beck, W. An, A. R. Lippert, J. C. Lewis and B. C. Dickinson, Development of a Split Esterase for Protein-Protein Interaction-Dependent Small-Molecule Activation, *ACS Cent. Sci.*, 2019, **5**, 1768–1776.
5 L. S. Ryan, A. Nakatsuka and A. R. Lippert, Photoactivatavle 1,2-dioxetane chemiluminophores, *Results Chem.*, 2021, **3**, 100106.
6 E. M. Digby, M. T. Tung, H. N. Kagalwala, L. S. Ryan, A. R. Lippert and A. A. Beharry, Dark Dynamic Therapy: Photosensitization without Light Excitation Using Chemiluminescence Resonance Energy Transfer in a Dioxetane–Erythrosin B Conjugate, *ACS Chem. Biol.*, 2022, **17**, 1082–1091.
7 L. Liu and R. P. Mason, Imaging β-Galactosidase Activity in Human Tumor Xenografts and Transgenic Mice Using a Chemiluminescent Substrate, *PLoS One*, 2010, **5**, e12024.
8 J. Cao, R. Lopez, J. M. Thacker, J. Y. Moon, C. Jiang, S. N. S. Morris, J. H. Bauer, P. Tao, R. P. Mason and A. R. Lippert, Chemiluminescent Probes for Imaging H_2S in Living Animals, *Chem. Sci.*, 2015, **6**, 1979–1985.
9 J. Cao, J. Campbell, L. Liu, R. P. Mason and A. R. Lippert, In Vivo Chemiluminescent Imaging Agents for Nitroreductase and Tissue Oxygenation, *Anal. Chem.*, 2016, **88**, 4995–5002.
10 S. Gnaim, O. Green and D. Shabat, The emergence of aqueous chemiluminescence: new promising class of phenoxy 1,2-dioxetane luminophores, *Chem. Commun.*, 2018, **54**, 2073–2085.
11 B. J. Bezner, L. S. Ryan and A. R. Lippert, Reaction-Based Luminescent Probes for Reactive Sulfur, Oxygen, and Nitrogen Species: Analytical Techniques and Recent Progress, *Anal. Chem.*, 2020, **92**, 309–326.
12 B. Li, Y. L. Kim and A. R. Lippert, Chemiluminescence measurement of Reactive Sulfur and Nitrogen Species, *Antioxid. Redox Signal.*, 2022, **36**, 337–353.
13 H. N. Kagalwala and A. R. Lippert, Energy Transfer Chemiluminescent Spiroadamantane 1,2-Dioxetane Probes for Bioanalyte Detection and Imaging, *Angew. Chem., Int. Ed.*, 2022, e202210057.
14 M. C. Cabello, G. Chen, M. J. Melville, R. Osman, G. D. Kumar, D. W. Domaille and A. R. Lippert, Ex Tenebris Lux: Illuminating Reactive Oxygen and Nitrogen Species with Small Molecule Probes, *Chem. Rev.*, 2024, **124**, 9225–9375.
15 Y. Wang, Y. Bian, X. Chen and D. Su, Chemiluminescent Probes Based on 1,2-Dioxetane Structures for Bioimaging, *Chem. – Asian J.*, 2022, **17**, e202200018.
16 A. P. Schaap, R. S. Handley and B. P. Giri, Chemical and Enzymatic Triggering of 1,2-Dioxetanes. 1: Aryl Esterase-catalyzed Chemiluminescence from a Naphthyl Acetate-Substituted Dioxetane, *Tetrahedron Lett.*, 1987, **28**, 935–938.
17 A. P. Schaap, T. S. Chen, R. S. Handley, R. DeSilva and B. P. Giri, Chemical and Enzymatic Triggering of 1,2-Dioxetanes. 2: Fluoride-induced Chemiluminescence from *tert*-Butyldimethylsilyloxy-substituted Dioxetanes, *Tetrahedron Lett.*, 1987, **28**, 1155–1158.
18 A. P. Schaap, M. D. Sandison and R. S. Handley, Chemical and Enzymatic Triggering of 1,2-Dioxetanes. 3: Alkaline Phosphatase-catalyzed Chemiluminescence from an Aryl Phosphate-substituted Dioxetane, *Tetrahedron Lett.*, 1987, **28**, 1159–1162.
19 J. Y. Koo and G. B. Schuster, Chemiluminescence of diphenoyl peroxide. Chemically initiated electron exchange

luminescence. A new general mechanism for chemical production of electronically excited states, *J. Am. Chem. Soc.*, 1978, **100**, 4496–4503.

20 L. H. Catalani and T. Wilson, Electron transfer and chemiluminescence. Two inefficient systems: 1,4-dimethoxy-9,10-diphenylanthracene peroxide and diphenoyl peroxide, *J. Am. Chem. Soc.*, 1989, **111**, 2633–2639.

21 L. Yue and Y. J. Liu, Mechanism of AMPPD Chemiluminescence in a Different Voice, *J. Chem. Theory Comput.*, 2013, **9**, 2300–2312.

22 L. F. M. L. Ciscato, F. H. Bartoloni, D. Weiss, R. Beckert and W. J. Baader, Experimental Evidence of the Occurrence of Intramolecular Catalyzed 1,2-Dioxetane Decomposition, *J. Org. Chem.*, 2010, **75**, 6574–6580.

23 W. Adam, I. Bronstein, A. V. Trofimov and R. F. Vasil'ev, Solvent-Cage Effect (Viscosity Dependence) as a Diagnostic Probe for the Mechanism of the Intramolecular Chemically Initiated Electron-Exchange Luminescence (CIEEL) Triggered from a Spiroadmantyl-Substituted Dioxetane, *J. Am. Chem. Soc.*, 1999, **121**, 958–961.

24 W. Adam and A. V. Trofimov, The Effect of *meta* versus *para* Substitution on the Efficiency of Chemiexcitation in the Chemically Triggered Electron-Transfer-Initiated Decomposition of Spiroadmantyl Dioxetanes, *J. Org. Chem.*, 2000, **65**, 6474–6478.

25 W. Adam, M. Matsumoto and A. V. Trofimov, Viscosity Dependence of the Chemically Induced Electron-Exchange Chemiluminescence Triggered from a Bicyclic Dioxetane, *J. Am. Chem. Soc.*, 2000, **122**, 8631–8634.

26 E. L. Bastos, S. M. da Silva and W. J. Baader, Solvent Cage Effects: Basis of a General Mechanism for Efficient Chemiluminescence, *J. Org. Chem.*, 2013, **78**, 4432–4439.

27 M. Khalid, M. A. Oliveira, S. P. Souza, L. F. M. L. Ciscato, F. H. Bartoloni and W. J. Baader, Efficiency of intermolecular chemiluminescence systems lacks significant solvent cavity effect in binary toluene/diphenylmethane mixtures, *J. Photochem. Photobiol.*, 2015, **312**, 81–87.

28 M. Khalid, S. P. Souza, Jr., L. F. M. L. Ciscato, F. H. Bartoloni and W. J. Baader, Solvent viscosity influence on the chemiexcitation efficiency of inter and intramolecular chemiluminescence systems, *Photochem. Photobiol. Sci.*, 2015, **14**, 1296–1305.

29 O. Green, T. Eilon, N. Hananya, S. Gutkin, C. R. Bauer and D. Shabat, Opening a Gateway for Chemiluminescence Cell Imaging: Distinctive Methodology for Design of Bright Chemiluminescence Dioxetane Probes, *ACS Cent. Sci.*, 2017, **3**, 349–358.

30 A. R. Lippert, Unlocking the Potential of Chemiluminescence Imaging, *ACS Cent. Sci.*, 2017, **3**, 269–271.

31 L. S. Ryan, J. L. Gerberich, J. Cao, W. An, B. A. Jenkins, R. P. Mason and A. R. Lippert, Kinetics-Based Measurement of Hypoxia in Living Cells and Animals Using an Acetoxymethyl Ester Chemiluminescent Probe, *ACS Sens.*, 2019, **4**, 1391–1398.

32 S. H. Li, G. R. Zhang, Y. T. He, L. Yang, H. L. Li, C. Y. Long, Y. Cui and X. Q. Wang, Emission Wavelength-Tunable Bicyclic Dioxetane Chemiluminescent Probes for Precise In Vitro and In Vivo Imaging, *Anal. Chem.*, 2023, **95**, 13191–13200.

33 M. Matsumoto, N. Watanabe, N. C. Kasuga, F. Hamada and K. Tadokoro, Synthesis of 5-Alkyl-1-aryl-4,4-dimethyl-2,6,7-trioxabicycli[3.2.0]heptanes as a Chemiluminescent Substrate with Remarkable Thermal Stability, *Tetrahedron Lett.*, 1997, **38**, 2863–2866.

34 W. A. Pryor, X. Jin and G. L. Squadrito, Insensitivity of the Rate of Decomposition of Peroxynitrite to Changes in Viscosity; Evidence against Free Radical Formation, *J. Am. Chem. Soc.*, 1996, **118**, 3125–3128.

35 S. Goldstein and G. Czapski, Viscosity Effects on the Reaction of Peroxynitrite with CO_2: Evidence for Radical Formation in a Solvent Cage, *J. Am. Chem. Soc.*, 1999, **121**, 2444–2447.

36 H. N. Kagalwala, J. Gerberich, C. J. Smith, R. P. Mason and A. R. Lippert, Chemiluminescent 1,2-Dioxetane Iridium Complexes for Near-Infrared Oxygen Sensing, *Angew. Chem., Int. Ed.*, 2022, **61**, e202115704.

37 A. K. Doolittle, Studies in Newtonian Flow. II. The Dependence of the Viscosity of Liquids on Free–Space, *J. Appl. Phys.*, 1951, **22**, 1471–1475.

38 A. Messaâdi, N. Dhoubi, H. Hamda, F. B. M. Belgacem, Y. H. Adbelkader, N. Ouerfelli and A. H. Hamzaoui, A New Equation Relating the Viscosity Arrhenious Temperature and the Activation Energy for Some Newtonian Classical Solvents, *J. Chem.*, 2015, 163262.

39 M. J. Goodwin, J. C. Dickenson, A. Ripak, A. M. Deetz, J. S. McCarthy, G. J. Meyer and L. Trojan-Gautier, Factors that Impact Photochemical Cage Escape Yields, *Chem. Rev.*, 2024, **124**, 7379–7464.

40 M. A. Haidekker and E. A. Theodorakis, Environment-sensitive behavior of fluorescent molecular rotors, *J. Biol. Eng.*, 2010, **4**, 11.

41 S. M. da Silva, A. P. Lang, A. P. F. dos Santos, M. C. Cabello, L. F. M. L. Ciscato, F. H. Bartoloni, E. L. Bastos and W. J. Baader, Cyclic Peroxidic Carbon Dioxide Fuels Peroxyoxalate Chemiluminescence, *J. Org. Chem.*, 2021, **86**, 11434–11441.

42 F. H. Bartoloni, M. A. de Oliveira, L. F. M. L. Ciscato, F. A. Augusto, E. L. Bastos and W. J. Baader, Chemiluminescence Efficiency of Catalyzed 1,2-Dioxetanone Decomposition Determined by Steric Effects, *J. Org. Chem.*, 2015, **80**, 3745–3751.

43 M. Khalid, S. P. Souza, M. C. Cabello, F. H. Bartoloni, L. F. M. L. Ciscato, E. L. Bastos, O. A. A. El Seoud and W. J. Baader, Solvent polarity influence on chemiexcitation efficiency of inter and intramolecular electron-transfer catalyzed chemiluminescence, *J. Photochem. Photobiol.*, 2022, **433**, 114161.